SINGLE NUCLEON COINCIDENCE CROSS SECTIONS IN A RELATIVISTIC MEAN FIELD THEORY*

By S. J. Pollock

Stanford University, Stanford, California, 94305, USA

and

Continuous Electron Beam Accelerator Facility, Newport News, VA, 23606, USA

(Received October 15, 1987)

We compute single nucleon emission cross sections in infinite nuclear matter within the context of a consistent, relativistic field theory with a conserved electromagnetic current. Special emphasis is placed on calculation of the 4 nuclear response functions, the full differential coincidence cross sections, the integrated singles cross section, and the Coulomb sum rule. Experimental inelastic cross sections can be used to fit the two free parameters in our theory for specific nuclei. Also, we analyze the kinematics required to measure the "out of plane" response functions.

PACS numbers: 21.65.+f

1. Introduction

Motivated by the possibility of a wide range of single nucleon emission measurements at the Continuous Electron Beam Accelerator Facility (CEBAF), we present some numerical predictions for coincidence cross sections. We work in a renormalizable, relativistic quantum field theory with meson and nucleon degrees of freedom [1] (called QHD-I). In particular, we use an infinite nuclear matter approximation to calculate the unpolarized nuclear response functions. This approximation gives a simple nuclear picture — it is a relativistic, shifted mass fermi gas. The theory is fully relativistic, allowing consistent calculations at arbitrary kinematics. It keeps the full relativistic vertex, and our electromagnetic current is explicitly conserved. In principle a more sophisticated approximation in the same general framework could be used to improve the calculations. However, this model may be useful as a first orientation for the future (e, e'N) coincidence programs at CEBAF.

Using the nuclear response functions, we compute full coincidence cross sections,

* Submitted by Prof. J. D. Walecka, member of the International Editorial Council of Acta Physica Polonica.

and also integrate over the ejected nucleon degrees of freedom to compute inelastic singles cross sections and the Coulomb sum rule. One emphasis of this calculation is to examine the contributions of the "out of plane" response functions, as this gives new information on hadronic nuclear matrix elements unobtainable in any singles experiment. In addition, we interpret the shape of the coincidence response functions in terms of a sampling of nucleon momenta throughout the fermi sphere.

2. *General form of the cross section*

The kinematics we consider are shown in Fig. 1. We write the matrix elements of the hadronic current as

$$J_\mu \equiv (\vec{J}, iJ_c) \equiv \frac{\sqrt{M_1 M_2}}{4\pi W}\left(\frac{2e_q E_1 E_2 \Omega^3}{M_1 M_2}\right)^{1/2} \langle p_2, q|J_\mu(0)\,|p_1\rangle. \tag{2.1}$$

Then, one can derive the exact result (to leading order in α) [2]:

$$\begin{aligned}\frac{d^5\sigma}{de_2 d\Omega_2 d\Omega_q} = \sigma_{\text{Mott}}&\left(\frac{M_1 q}{\pi W}\right)\\ &\times\left\{\frac{k^4}{k^{*4}}|J_c|^2\right.\\ &+\left(\frac{k^2}{2k^{*2}}+\frac{W^2}{M_1^2}\tan^2(\theta/2)\right)(|J^{+1}|^2+|J^{-1}|^2)\\ &+\frac{k^2}{2k^{*2}}\cdot 2\,\text{Re}\,(J^{+1})^*(J^{-1})\\ &\left.+\frac{k^2}{k^{*2}}\left(\frac{k^2}{k^{*2}}+\frac{W^2}{M_1^2}\tan^2(\theta/2)\right)^{1/2}\sqrt{2}\,\text{Im}\,J_c^*(J^{+1}+J^{-1})\right\}\end{aligned} \tag{2.2}$$

where the Mott cross section is

$$\sigma_{\text{Mott}} = \frac{4\alpha^2 e_2^2\cos^2(\theta/2)}{k^4},$$

and k^* is the virtual photon 3 momentum, W the total energy, and q the outgoing nucleon's momentum, in the center of momentum frame. E_1 (M_1) and E_2 (M_2) are the initial and final recoil nucleus energies (masses), e_2 is the final electron energy in the lab, and θ_2 (Ω_2) the electron scattering angle (solid angle) in the lab. We quantize in a large box of volume Ω. The superscripts refer to the helicity components of $\vec{J}$:

$$J^{\pm 1} = \pm\frac{1}{\sqrt{2}}(J_1 \pm iJ_2).$$

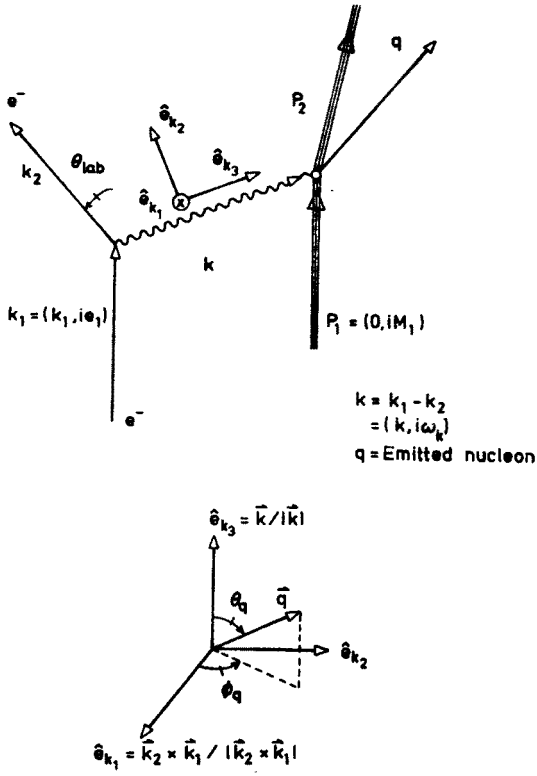

Fig. 1. Kinematics and conventions for coincidence cross sections

For infinite nuclear matter, the center of momentum frame is equivalent to the lab frame, and the M_1's and W's drop out. The first line in the brackets, above, yields the longitudinal response function familiar from singles cross sections. The second line gives the transverse response, while the last two lines are new. In fact one can show quite generally [3] that their azimuthal dependence is explicitly given by

$$T_3 \equiv \frac{k^2}{2\vec{k}^2} \cdot 2\,\mathrm{Re}\,(J^{+1})^*(J^{-1}) \propto \cos 2\phi_q$$

$$T_4 \equiv \frac{k^2}{\vec{k}^2}\left(\frac{k^2}{\vec{k}^2} + \frac{W^2}{M_1^2}\tan^2(\theta/2)\right)^{1/2} \sqrt{2}\,\mathrm{Im}\,J_c^*(J^{+1} + J^{-1}) \propto \sin\phi_q \qquad (2.3)$$

with ϕ_q as defined in Fig. 1. Thus we see that with purely in-plane experiments ($\vec{q}$ lies in the scattering plane, so $\phi_q = \pm\pi/2$) we can not isolate the term T_3.

3. Mean field theory

In QHD-I, we have a nucleon field ψ, a scalar meson field ϕ, and a vector meson field V_μ. In the mean field approximation, these field operators are replaced by their expectation values, which are classical fields. In infinite nuclear matter, these become con-

stants, independent of $\vec{x}$. In this case, the equation for the nucleon fields can be solved exactly, and just give "free" Dirac spinors with shifted mass m^* and shifted energy. The energy shift cancels in differences, and thus our model is a relativistic Fermi gas of nucleons with mass m^* (see Ref. [1]).

Figure 2 shows the kinematics in this case. We note that in this model ω_k is determined

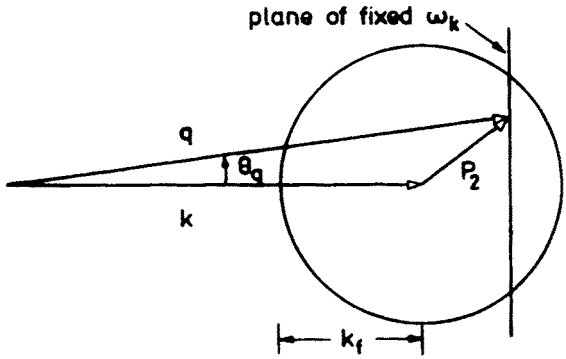

Fig. 2. Picture of the scattering in this model. The incoming virtual photon has momentum $\vec{k}$, the struck nucleon has momentum $-\vec{p}_2$, and the outgoing nucleon has momentum $\vec{q}$. Note that the *ejected* nucleon still has an effective mass m^*, since the nucleus is infinite

by the magnitudes of the nucleon 3-momentum and the "missing", or hole momentum:

$$\omega_k = \sqrt{\vec{q}^2 + m^{*2}} - \sqrt{\vec{p}_2^2 + m^{*2}}.$$

This simplification of kinematics is a consequence of our Fermi gas model[1]. Note also that it is clear from Fig. 2 that, given a fixed $\vec{k}$, ω_k has sharp maximum and minimum cutoffs. Also indicated in the figure is the fact that a variety of $\vec{q}$, $\vec{p}_2$ combinations, namely those which end up in the plane perpendicular to $\vec{k}$, all yield the same energy loss. (In the nonrelativistic limit this surface is a plane, in general it is a bit more complicated.) Given an energy loss ω_k, and virtual photon momentum $\vec{k}$, one sees from the diagram that there are a range of θ_q's allowed, and as θ_q runs from zero to its maximum value, we are sampling different regions of the Fermi sphere, from the center out to the edge. This is a nice physical picture in which to interpret response functions and cross sections plotted as functions of ω_k and $\cos\theta_q$. At fixed energy loss, the θ_q dependence is just "mapping out" the Fermi sphere.

In order to calculate the response functions in this model, we also must assume a form for the electromagnetic current operator. For a *free* nucleon

$$\langle p'|J_\mu(0)|p\rangle = \frac{i}{\Omega}\bar{u}(p')\left[F_1(k^2)\gamma_\mu + F_2(k^2)\sigma_{\mu\nu}k_\nu\right]u(p),$$

where $F_1(k^2)$ and $F_2(k^2)$ are the usual single nucleon form factors. For the current matrix

[1] Here the outgoing nucleon has shifted mass m^*. Of course, the *observed* nucleon in a coincidence experiment has left the "infinite" nuclear matter, but its final laboratory energy is well defined, since the fermi energy is determined on an absolute scale by the nuclear binding energy.

elements in the mean field model (in the rest frame of the nucleus), we use

$$\langle p_2, q|J_\mu(0)|p_1\rangle = \frac{i}{\Omega}\bar{u}(q)\,(F_1(k^2)\gamma_\mu + F_2(k^2)\sigma_{\mu\nu}k_\nu]u(-p_2)$$

$$\times\theta(|\vec{q}|-k_f)\theta(k_f-|\vec{p}_2|)\delta(\omega_k-(e_q-e_{p2})). \tag{3.1}$$

This comes from assuming an effective current operator [1] which is conserved, covariant, and reproduces the structure of the free nucleon. The structure functions then come from simple trace calculations (see appendix A).

4. Results

4.1. Coincidence cross sections

The response functions for a particular choice of electron kinematics are shown in Figure 3. In each set, they are plotted with identical scales to show their relative sizes.

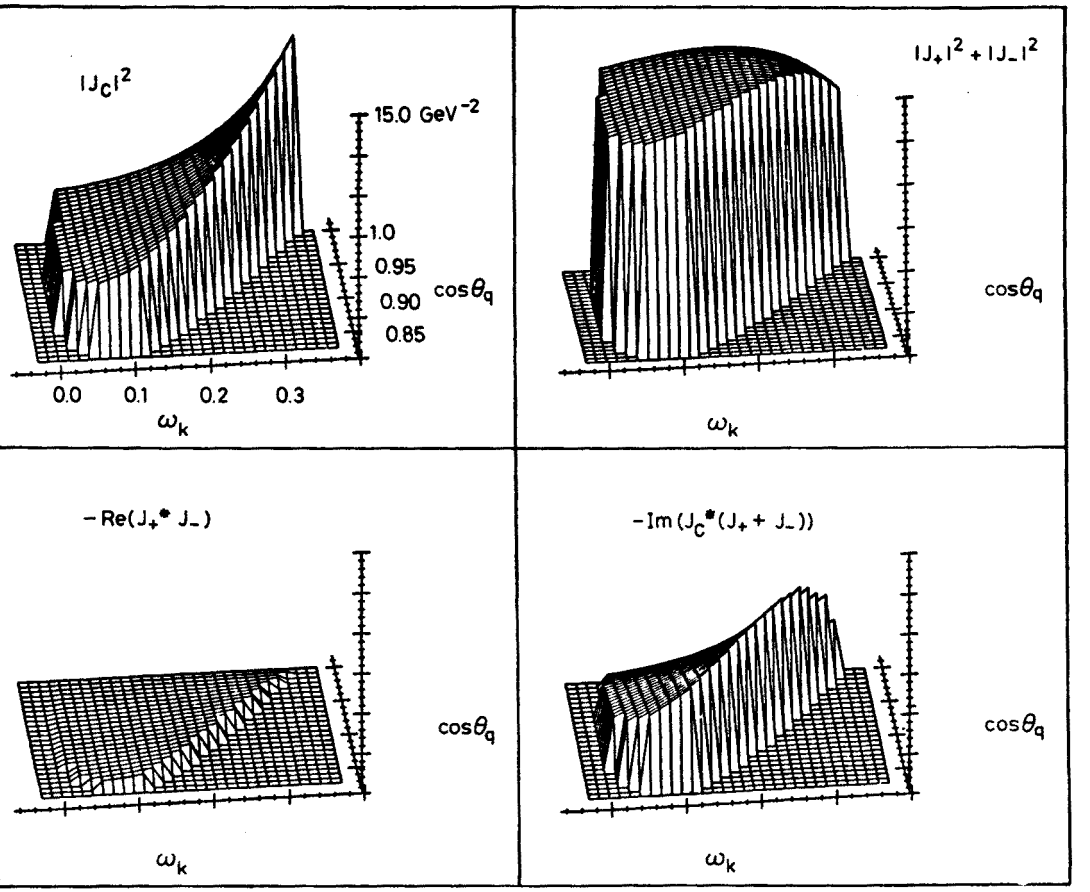

Fig. 3a

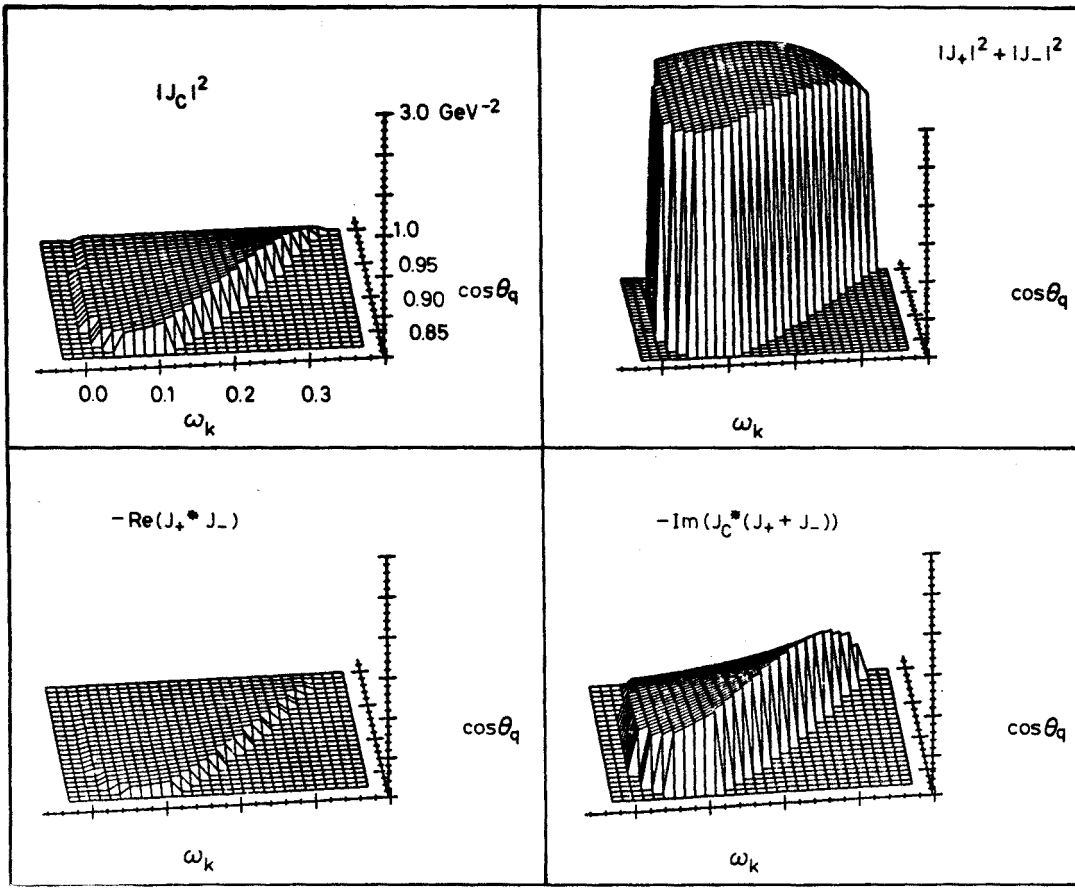

Fig. 3b

Fig. 3a) The four proton response functions evaluated per proton, and plotted as functions of energy loss and cos θ_q. Here $\vec{k} = 0.5$ GeV and $\theta_q = \pi/2$. We use $k_f = 0.28$ GeV and $m^*/m = 0.56$ (appropriate for infinite nuclear matter [1]). The vertical scale is 15.0 GeV^{-2} for all four response functions. b) Neutron response functions (per neutron). The vertical scale is magnified over Fig (a) by a factor of 5

Note that a slice at fixed ω_k gives the dependence of the response functions on the scattered nucleon's initial momentum in the Fermi sea, as discussed in Section 2. As θ_q varies from 0 out to its maximum, we are scattering from nucleons lying progressively further from the center of the Fermi sphere. We show a typical differential cross section curve in Fig. 4. For this plot we have integrated over azimuthal angle to get a "ϕ averaged" coincidence cross section. Note that neither of the last two structure functions contribute after integrating over ϕ_q. In this plot, the relation of the coincidence cross section to the singles cross section is clear. At a fixed energy loss, the singles cross section is just the area under the slice. Thus, even just considering the "ϕ averaged" cross section, where the two new structure functions do not contribute at all, we can see the significance of coincidence measurements: they provide a mapping of the momentum distribution of the nucleons in the nucleus.

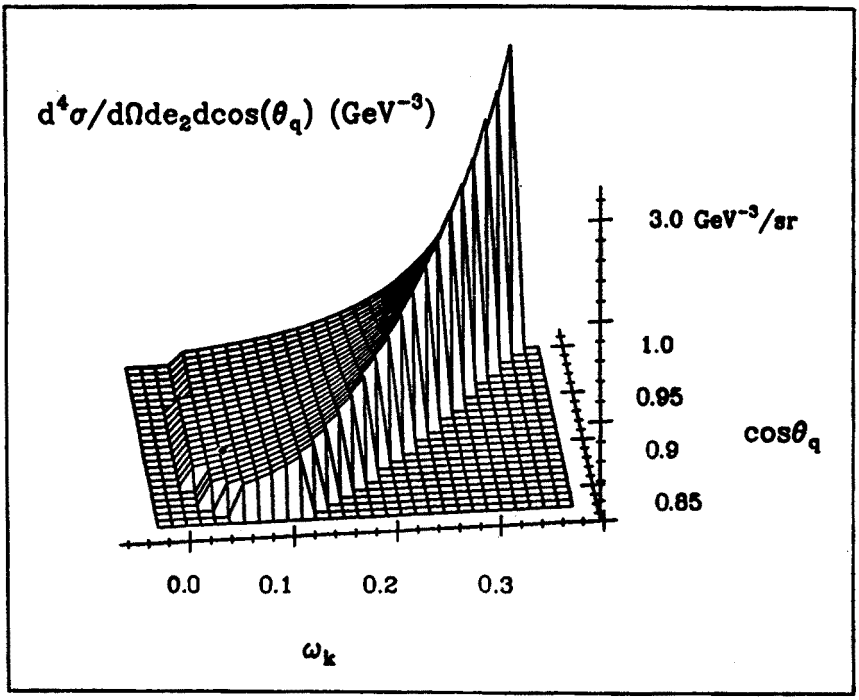

Fig. 4. Three dimensional plot of the proton coincidence cross section (per nucleon) integrated over the outgoing proton's azimuthal angle ϕ_q, $d^4\sigma/d\Omega de_2 d\cos\theta_q$. The electron kinematics and independent variables are the same as in the last figure, with $e_1 = 4.0$ GeV. The cross section is plotted on the z axis, and ranges from 0.15 GeV^{-3}/sr to 3.51 GeV^{-3}/sr

4.2. Singles cross sections

Figure 5 is a plot of the full singles inelastic cross section, including both proton and neutron emission. We have fit k_f and m^* to experimental data. Note that there is no arbitrary binding energy put in to fit the data — we only have the two infinite nuclear matter parameters to change. In Figure 6 we show the results of fitting several different nuclei. Note that in the smaller nuclei, our fitted Fermi momentum is lower than its value for infinite nuclear matter. In more sophisticated approximations (e.g. Thomas Fermi, or Hartree calculations) the Fermi energy would be dependent on radius, decreasing at the surface where the nuclear density falls off [1]. In our model with no radial dependences, this results in an overall reduction of the Fermi momentum. As nuclei get larger, the surface becomes less important, and the average Fermi momentum approaches its value for infinite nuclear matter. This is clearly demonstrated in Figure 6. Similarly, the effective mass m^* should approach m at the surface, so the value we obtain for m^*/m is closer to 1 for small nuclei, and approaches its asymptotic infinite nuclear matter value as A increases.

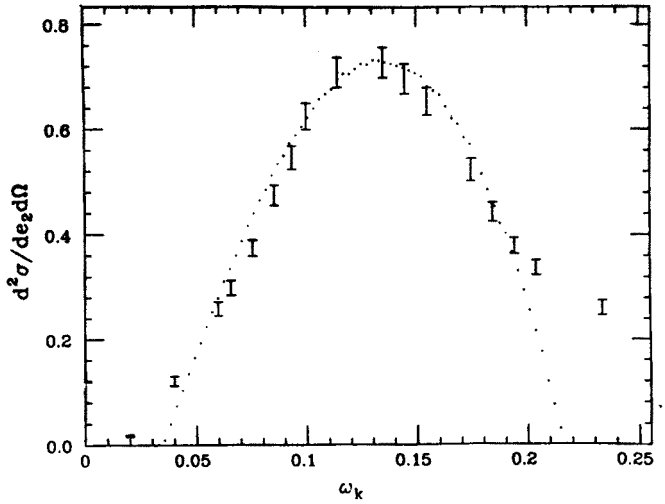

Fig. 5. Inelastic singles cross section for ^{12}C in units of 10^{-32} cm^2/sr/Mev, as a function of energy loss. Beam energy is $e_1 = 0.5$ GeV, electron scattering angle is $\theta = 60°$. The data is taken from Ref. [4]. The fit ($k_f = 0.19$ GeV, $m^*/m = 0.725$, here) is by eye

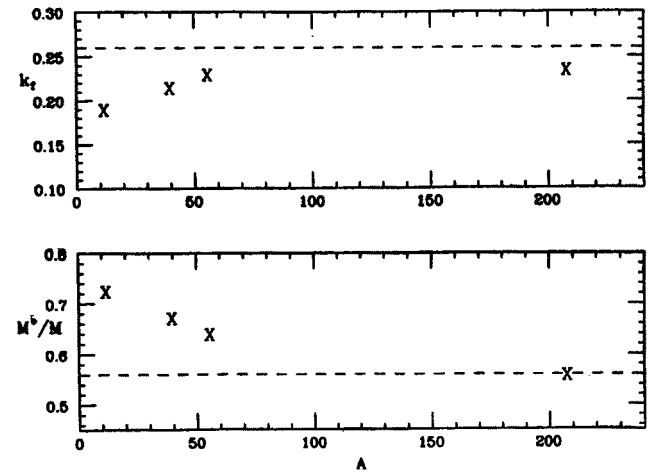

Fig. 6. Fitted Fermi energy and effective mass, as functions of Atomic number. The fits are described in the previous figure. Here, for infinite nuclear matter values we show a value of $k_f = 0.26$ GeV which reproduces the interior charge density of lead in the Hartree approximation

4.3. Sum rule

Figure 7 shows the integrated longitudinal sum rule. This is defined as

$$S_L(\vec{k}) = \int d\omega \frac{\vec{k}^4}{k^4} \frac{1}{\sigma_{\text{Mott}}} \left(\frac{d^2\sigma^{\text{Coul.}}}{d\Omega_2 de_2} \right). \tag{4.1}$$

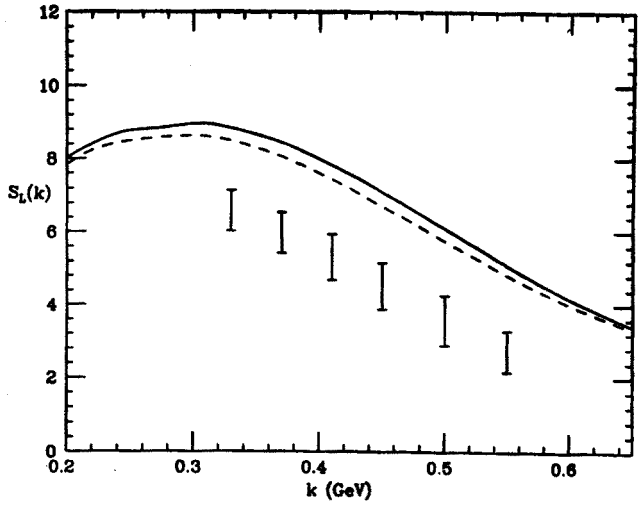

Fig. 7. The longitudinal sum rule for ^{40}Ca evaluated from equation (4.1). Data is from Ref. [8]. The solid curve is $m^* = 1.0$, the dashed curve is $m^* = 0.56$

Note that with this definition, the sum rule is *not* normalized to Z at high momentum transfers (even in the nonrelativistic limit) since there are single nucleon form factors buried in the differential cross section. We observe that the data lie significantly below our calculations. It is unclear what the origin of the discrepancy between theory and experiment is, although finite nucleus effects may be important [5].

Relation to previous work on the sum rule. There has been some discussion of the Coulomb sum rule in the literature [6, 7], and it is interesting to see how our calculations compare with others. A modified sum rule is often defined by

$$S(\vec{k}) = \int d\omega \frac{\vec{k}^4}{k^4} \frac{1}{\bar{\sigma}_{\text{Mott}}} \left(\frac{d^2\sigma^{\text{Coul.}}}{d\Omega_2 de_2} \right). \tag{4.2}$$

Here the modified Mott cross section $\bar{\sigma}_{\text{Mott}}$ *includes* the square of the single nucleon dipole form factor

$$\bar{\sigma}_{\text{Mott}} = \sigma_{\text{Mott}} g_D^2,$$

$$g_D = \frac{1}{(1+k^2/0.71)^2}. \tag{4.3}$$

Using this definition, the theoretical non-relativistic sum rule just gives the total nuclear charge Z for large momentum transfers. This is in fact modified when using our full effective current (3.1) which includes anomalous magnetic moments. Within the context of a relativistic mean field theory, the full sum rule can still be theoretically calculated, and is of course no longer just Z [6]. However, it is important to note the kinematically accessible sum rule (KAS), the sum rule *measurable* in electron scattering experiments, is only integrated

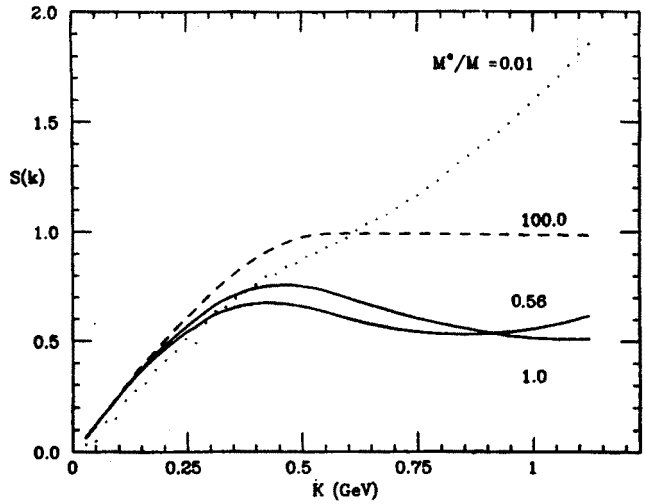

Fig. 8. Coulomb sum rule found by numerically integrating Eq. (4.2) over kinematically accessible energy loss. The dashed line results from setting $m^* = 100$. This reproduces the nonrelativistic sum rule, which is just 1 for $\vec{k} \geqslant 2k_f$. The other curves are for values of $m^*/m = 0.01$, 0.56, 0.7, and 1. For this plot, we assume a dipole dependence for F_1 and F_2, rather than G_M and G_E

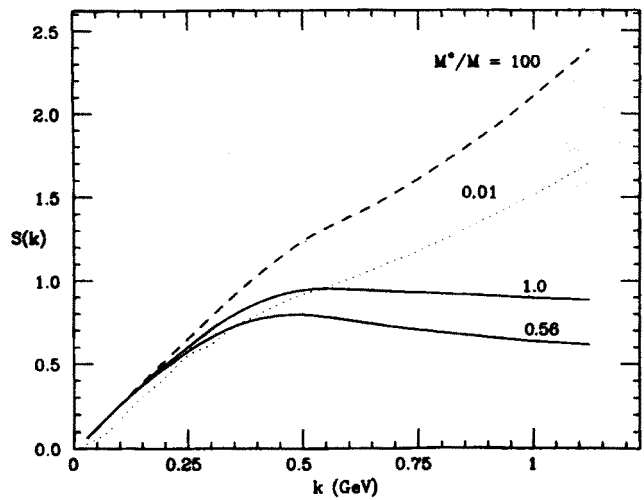

Fig. 9. Same as previous Figure, but assuming a dipole dependence for G_M and G_E rather than F_1 and F_2

up to the maximum kinematically available energy loss $\omega = |\vec{k}|$. One consequence of this is that the timelike contribution to the theoretical sum rule does not contribute to the KAS [7]. This timelike piece can be quite significant, and does *not* vanish for large momentum transfers. The KAS is in fact much reduced from the nonrelativistic prediction. In Figure 8 we plot the Coulomb sum rule (4.2) for various values of effective mass m^*. To compare with previous references, we assume a direct dipole dependence for the single

nucleon form factors F_1 and F_2, which breaks down at higher momentum transfers [9]. In Figure 9 we present the same calculation, only assuming a dipole dependence for G_M and G_E, which is a more accurate representation of the data [9]. Note that this makes a rather significant change, implying that the sum rule is quite sensitive to the nucleons' structure. To understand this change, note that a simple dipole fit for G_M and G_E yields e.g.

$$F_1^{\text{prot}} = g_D \frac{(1+\mu_p k^2/4m_p^2)}{(1+k^2/4m_p^2)}$$

(rather than just $F_1^p = g_D$), so that at $\vec{k} = 1$ GeV, (for ω small) $F_1^p \approx g_D \times 1.4$, a very substantial change, caused by the anomalous magnetic moment of the proton [6].

4.4. Out of plane response functions

The last two terms in the cross section (2.2), T_3 and T_4, have the explicit azimuthal dependences indicated in Eq. (2.3). Both of these "out of plane" response functions contribute maximally when $\phi_q = \pm\pi/2$, where the outgoing nucleon is in fact *in* the electron scattering plane. (See Fig. 1). When ϕ_q goes from $+\pi/2$ to $-\pi/2$, the term T_4 changes sign and so can be isolated from purely in-plane measurements. However, T_3 does not change sign, and thus can only be separated by making out of plane measurements. As seen in Fig. 3, this response function is very small in the infinite nuclear matter approximation. We have performed a kinematics search in order to find the conditions which optimize its contribution. For a few different beam energies, and electron scattering angles, we have

TABLE I

Out of plane structure function contributions

e_1	θ_e	ω_k	$\cos\theta_q$	$T_3/(T_1+T_2)$	α
4 GeV	10°	0.386	0.9417	7.6%	3.7°
	20°	1.15	0.986	4.9%	3.9°
	90°	3.44	0.9977	0.6%	4.0°
2.5 GeV	10°	0.16	0.8625	8.5%	5.2°
	20°	0.513	0.96	6.5%	5.9°
	90°	1.99	0.994	1.0%	6.4°
1 GeV	10°	0.029	0.563	9.7%	8.3°
	20°	0.06	0.717	8.8%	13.8°
	90°	0.613	0.967	2.1%	15.8°

T_i here refers to the i^{th} line in the cross section formula. Thus e.g.

$$T_3 \equiv (k_\mu^2/2\vec{k}^2)2 \text{ Re } (J^{+*}J^-).$$

Note that in each row, with e_1 and θ_e fixed, we have *chosen* both ω_k and θ_q to maximize the contribution of T_3. We consider small angles for θ_e (10, 20°) since the out of plane response is enhanced there, and include a larger angle (90°) for comparison. α is the incident beam bend angle required at these particular kinematics, in order to result in $\phi_q = 0$ (i.e. maximally out of plane), as discussed in Appendix B. Note also that the physical electron spectrometer angle θ_1 differs from θ_e slightly.

evaluated the fractional contribution of the third term to the "ϕ averaged" cross section over the entire allowed range of energy loss and nucleon scattering angle. We present the particular values which maximized this contribution in Table I. It appears that small electron scattering angles and lower beam energies increase its contribution. There is, however, an experimental constraint which favours high beam energy. A likely experimental setup will have the two spectrometers in a plane, and out of plane measurements will be made by bending the incident electron beam direction. The required beam bend is calculated in Appendix B, and tabulated in Table I. This bend angle gets large as beam energy drops, thus preventing us from going to very low energies to measure the out of plane response function. In general, the term T_3 is quite small, and even under optimal conditions is at most less than 10% of the total cross section. In other nuclear models, this response function may not be so small [10], and hence would be an extremely interesting quantity to measure.

5. *Summary*

We have calculated the four response functions for single nucleon emission in a mean field theory of nuclear matter. We show representative plots, including the full coincidence cross sections, integrated singles cross sections, and the Coulomb sum rule. Our model is fully relativistic, with a conserved current, and our calculations can therefore be done for any kinematics. While more sophisticated models certainly exist [11], it is instructive to see what basic physics we can extract from a physically clear relativistic Fermi gas calculation. We reproduce singles cross sections quite well, although the sum rule indicates a possible breakdown of the model. Nevertheless, we produce general guidelines for expected cross sections, and kinematical requirements such as minimum incident beam bend capability, and energies.

The author would like to thank Prof. J. D. Walecka for valuable discussions, comments, and suggestions. The author would also like to thank CEBAF for its hospitality, and use of computer on which the numerical calculations were made.

APPENDIX A

Derivation of the structure functions

If the initial and final target polarization are not observed, the four terms in the cross section can all be immediately obtained as components of the general response tensor $\sum_{i,f} J_\mu^* J_\nu$ with J_μ given by equation (2.1)[2]. Pulling out an overall normalization factor N, we want

$$\sum_{i,f} J_\mu^* J_\nu = |N|^2 \sum_{i,f} |\bar{u}(q)\,[F_1\gamma_\mu + F_2\sigma_{\mu\nu}k_\nu]u(p)|^2,$$

[2] In fact, one can quite easily extend Eq. (2.2) to take into account the possibility of polarized electron beams. However, the new helicity dependent response function which appears turns out to be zero in this model, as there are no final state interactions.

where $p_\mu \equiv (-\vec{p}_2, e_2) = q_\mu - k_\mu$. But this is extremely similar to the usual structure function in the Rosenbluth formula for elastic e-p scattering [12]. Keeping in mind that our spinors have a mass m^*, we can then immediately read off from the Rosenbluth formula:

$$\sum_{i,f} J_\mu^* J_\nu = |N|^2 \frac{2}{e_p e_q}\left(\frac{k_\mu^2}{4}(F_1+2m^*F_2)^2\left(\delta_{\mu\nu}-\frac{k_\mu k_\nu}{k^2}\right)\right.$$

$$\left.+(F_1^2+k_\mu^2 F_2^2)\,(p_\mu+\tfrac{1}{2}k_\mu)\,(p_\nu+\tfrac{1}{2}k_\nu)\right),$$

with $e_p \equiv \sqrt{\vec{p}_2^{\,2}+m^{*2}}$; $\quad e_q \equiv \sqrt{\vec{q}^{\,2}+m^{*2}}$; $\quad (p_\mu+\tfrac{1}{2}k_\mu) = (q_\mu-\tfrac{1}{2}k_\mu)$; $\quad k_4 = i\omega_k$, etc. So

$$|J_c|^2 = \sum_{i,j} J_4^* J_4$$

$$= \frac{-2|N|^2}{e_p e_q}\left[(F_1+2m^*F_2)^2\frac{\vec{k}^2}{4}-(F_1^2+k_\mu^2F_2^2)\,(e_q-\tfrac{1}{2}\omega_k)^2\right]$$

$$|J^{+1}|^2+|J^{-1}|^2 = \sum_{i,f}(|J_1|^2+|J_2|^2)$$

$$= \frac{2|N|^2}{e_p e_q}\left[(F_1+2m^*F_2)^2\frac{k_\mu^2}{2}+(F_1^2+k_\mu^2F_2^2)\,(q_1^2+q_2^2)\right]$$

$$\mathrm{Re}\,(J^{+1})^*(J^{-1}) = \sum_{i,j}\tfrac{1}{2}(|J_2|^2-|J_1|^2)$$

$$= \frac{2|N|^2}{e_p e_q}\left[(F_1^2+k_\mu^2F_2^2)\frac{(q_2^2-q_1^2)}{2}\right]$$

$$\mathrm{Im}\,J_c^*(J^{+1}+J^{-1}) = \sum_{i,f} -\sqrt{2}\,\mathrm{Im}\,J_2^*J_4$$

$$= -\sqrt{2}\,\frac{2|N|^2}{e_p e_q}\,[(F_1^2+k_\mu^2F_2^2)\,(e_q-\tfrac{1}{2}\omega_k)q_2].$$

To define $|N|$, note that in writing equation (2.2) we have implicitly included a phase space integral over the magnitude of the outgoing momenta, absorbing our overall energy conserving delta function [12], and using

$$\int d\vec{q}\,d\vec{p}_2\,\delta^4(k_1+p_1-k_2-p_2-q) = \frac{qe_qE_2}{W}\,d\Omega_q; \qquad \text{CM frame}$$

In the case of infinite nuclear matter, E_2 and W are both infinite, and we instead need to use an infinite nuclear matter phase space integral

$$\int d\vec{q}\,d\vec{p}_2\,\delta^4(k_1+p_1-k_2-p_2-q)$$

$$= \int d\vec{q}\,\delta(\omega_k-\sqrt{q^2+m^{*2}}-\sqrt{(\vec{q}-\vec{k})^2+m^{*2}})$$

$$= qe_q d\Omega_q\left[\frac{e_p}{e_p-e_q(1-\vec{k}\cdot\vec{q}/q^2)}\right],$$

and thus combining with equations (2.1) and (2.2) gives

$$|N|^2 = \frac{2e_q\Omega}{(4\pi)^2}\left[\frac{e_p}{e_p - e_q(1-\vec{k}\cdot\vec{q}/q^2)}\right].$$

$\Omega = 3\pi^2 Z/k_f^3$ comes from normalizing a fermi gas of Z particles in a volume Ω.

In our numerical calculations, we obtain the free proton form factors F_1 and F_2 by assuming a dipole dependence for the Sachs electric and magnetic form factors. In particular:

$$G_M^{p,n}(k^2) \equiv F_1^{p,n} + 2M_{free}F_2^{p,n} = G_M^{p,n}(0)g_D(k^2),$$

$$G_E^{p,n}(k^2) \equiv F_1^{p,n} - \frac{k_\mu^2}{2M_{free}}F_2^{p,n} = G_E^{p,n}(0)g_D(k^2),$$

where $M_{free} = 0.938$ GeV is the free space nucleon mass, $G_M^{p,n}(0) = \mu^{p,n}$ are the free nucleon magnetic moments, $G_E^{p,n}(0) = 1, 0$ are the nucleon charges, and $g_D(k^2)$ is given by Eq. (4.3).

APPENDIX B

Out of plane kinematics

The out of plane structure functions require measurements at $\phi_q \neq \pm\pi/2$. To achieve this, one can either move the proton spectrometer out of plane, or bend the incident beam out of plane. The kinematics in this latter case are shown in Fig. 10. Note that the *kinematics* is not changed, only the notation and definitions of angles. In this case, the electron

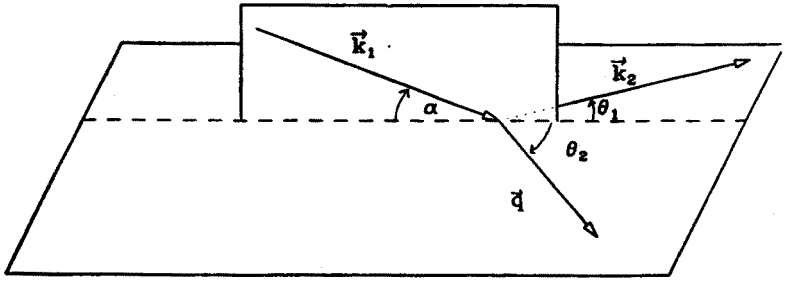

Fig. 10. Out of plane kinematics definitions. See Appendix B

spectrometer is set at angle θ_1 from the incident beam's forward direction. The beam bend angle α is given by:

$$\sin\alpha = \frac{-\sin\theta\sin\theta_q\cos\phi_q}{\sqrt{\sin^2\theta_q\cos^2\phi_q + \frac{1}{\vec{k}^2}[e_1\sin\theta\cos\theta_q + (e_2 - e_1\cos\theta)\sin\theta_q\sin\phi_q]^2}},$$

In the case of maximum out of plane scattering, $\phi_q = 0$ and this reduces to

$$\sin \alpha = \frac{-\sin \theta \sin \theta_q}{\sqrt{\sin^2 \theta_q + \frac{e_1^2}{\vec{k}^2} \sin^2 \theta \cos^2 \theta_q}}.$$

The electron spectrometer angle θ_1 is related to the true angle between incident and final electron θ by

$$\cos \theta_1 = \frac{\cos \theta}{\cos \alpha}.$$

REFERENCES

[1] B. Serot, J. D. Walecka, *The Relativistic Nuclear Many-Body Problem*, Advances in Nuclear Physics, Vol. 16, 1986.

[2] P. L. Pritchett, J. D. Walecka, P. A. Zucker, *Phys. Rev.* **184**, 1825 (1969).

[3] W. E. Kleppinger, J. D. Walecka, *Ann. Phys.* **146**, 349 (1983).

[4] R. R. Whitney et al., *Phys. Rev.* **C9**, 2230 (1974).

[5] H. Kurasawa, T. Suzuki, *Phys. Lett.* **B173**, 377 (1986); K. Wehrberger, F. Beck, *Phys. Rev.* **C35**, 298 (1987).

[6] J. D. Walecka, *Nucl. Phys.* **A399**, 387 (1983).

[7] T. Matsui, *Phys. Lett.* **132B**, 260 (1983); T. DeForest jr., *Phys. Lett.* **152B**, 151 (1985); G. Dang, M. L'Huillier, N. Van Giai, J. Van Orden, Univ. Paris, Orsay preprint IPNO/TH 86-78.

[8] Z. Meziani et al., *Phys. Rev. Lett.* **52**, 2130 (1984).

[9] W. Bartel et al., *Nucl. Phys.* **B58**, 429 (1973).

[10] H. Arenhövel, *Nucl. Phys.* **A358**, 263 (1981), which includes meson exchange and isobar contributions. These have a large affect on R_{TT} in the case of a deuteron target.

[11] S. Boffi, C. Grusti, F. D. Pacati, *Nucl. Phys.* **A386**, 599 (1982) (also 1986 CEBAF Summer Workshop, June 23–27, 1986, p. 133); A. Picklesimer, J. W. Van Orden, S. J. Wallace, *Phys. Rev.* **C32**, 1312 (1985).

[12] J. D. Walecka, in *Electron Scattering Notes*, ANL-83-50; M. N. Rosenbluth, *Phys. Rev.* **79**, 615 (1950).